Weld Cracking in Duplex Stainless Steel (Report III)†

— Numerical Analysis on Solidification Brittleness Temperature Range in Stainless Steel —

Fukuhisa MATSUDA*, Hiroji NAKAGAWA** and Jong-Bong LEE***

Abstract

Two dimensional modelling of the cellular dendritic growth during weld solidification was applied to predict Solidification Brittleness Temperature Range (BTR) of several kinds of stainless steels. The calculation of BTR was done based on the observation that the lower temperature limit of BTR corresponds to the temperature in which residual liquid enriched with impurities solidifies completely. This treatment gave a good agreement between the calculated and the experimental BTR for ferritic and fully austenitic stainless steel by paying attention to mesh size in the model. Moreover, the treatment was also useful to rank harmful elements in crack susceptibility. Then, the modelling was applied to predict the reason why duplex stainless steel has a relatively large BTR, and consequently it was judged through calculation that nitrogen is very harmful. This prediction was confirmed experimentally by making tentative deposited metal containing low nitrogen.

Therefore, the calculation is very useful to predict or analyze BTR for materials which solidifies as single phase. However, the calculation has a limit for the application to materials in which peritectic/eutectic reation occurs.

KEY WORDS: (Computation) (Hot Cracking) (Solidification) (Stainless Steels)

1. Introduction

In the previous paper[1], the authors made two dimensional modelling of cellular dendritic growth during weld solidification. The calculated results by the modelling fitted well with the observed results in the problems of microsegregation and the temperature where the solid bridge is formed due to the mutual contact of the tips of secondary dendrite arms.

Such a good correspondence between the modelling results and the experimental results aroused a hope to predict Solidification Brittleness Temperature Range (BTR) during welding, which is one of the most important indices to evaluate crack susceptibility[2,3] and can be measured easily by the Trans-Varestraint test. One of the advantage of BTR is that it has a definite physical meaning as follows: On SEM fractograph of solidification crack made by the Trans-Varestraint test[4,5], a change in situation of traces of residual liquid on grain boundary can be seen from the liquidus temperature to the lower temperature limit of BTR, except for the material which has a peritectic/eutectic reaction. According to the detailed observation of the traces, it was judged[4] that the lower temperature limit of BTR corresponded to the temperature where small amount of residual liquid enriched with impurity elements solidified completely. If it is general, the prediction of BTR by the modelling will be easy.

Another advantage of the prediction of BTR by the modelling is that ranking of harmful elements should be possible, because any kinds of probably influential elements can be numerically analyzed simultaneously in one analysis. This aroused another hope to find out the reason why duplex stainless steel is rather susceptible to weld solidification cracking.

Therefore, the procedure to predict BTR and the accompanying problems are discussed in this paper, and finally the reason of high crack susceptibility of duplex stainless steel is pursued and confirmed experimentally.

2. Materials and Experimental Procedures Used

2.1 Materials used

The chemical compositions of commercial stainless steels used are shown in **Table 1**, where SUS316L and SUS304L are used as representatives of material having peritectic/eutectic reaction[6,7]. The chemical compositions of deposited metals made are shown in **Table 2**. These were made to confirm a predicted harmful effect of nitrogen on solidification crack in duplex stainless steel, and the procedure to make the deposited metal is shown elsewhere[8].

† Received on May 8, 1989
* Professor
** Instructor
*** Graduate Student

Transactions of JWRI is published by Welding Research Institute of Osaka University, Ibaraki, Osaka 567, Japan

Table 1 Chemical compositions of base metals of commercial stainless steel used.

Material	Chemical composition (wt.%)										Thickness
	C	Si	Mn	P	S	Cr	Ni	Mo	N	Others	(mm)
SUS329J2L	0.017	0.57	1.57	0.028	0.001	22.13	5.49	2.92	0.14	Cu:0.07	12.0
SUS310S	0.070	0.61	1.67	0.022	0.001	24.78	19.14	0.06	0.03	O:0.006	12.0
SUS316L	0.025	0.58	1.12	0.012	0.003	16.92	13.98	2.10	-	-	1.5
SUS304L	0.020	0.59	0.99	0.028	0.013	19.09	9.75	0.08	-	-	2.0
SUS430	0.070	0.64	0.57	0.027	0.005	16.24	0.42	0.05	0.01	-	12.0

Table 2 Chemical compositions of tentative deposited metals to confirm harmful effect of nitrogen on solidification crack in duplex stainless steel.

Mark	Chemical composition (wt.%)										Ferrite*
	C	Si	Mn	P	S	Cr	Ni	Mo	O	N	(%)
DP-70HN	0.031	0.65	0.96	0.026	0.006	24.26	4.75	2.94	0.019	0.107	77
DP-80HN	0.037	0.55	1.19	0.021	0.007	24.17	6.93	2.66	0.062	0.112	77
DP-100HN	0.040	0.51	1.20	0.022	0.007	24.63	2.35	2.81	0.062	0.118	99
DP-5LN	0.020	0.61	1.27	0.019	0.008	24.03	19.15	2.69	0.031	0.037	3
DP-70LN	0.017	0.62	1.25	0.020	0.009	24.20	10.83	2.82	0.026	0.036	77
DP-80LN	0.016	0.63	1.25	0.021	0.008	23.85	9.98	2.73	0.028	0.036	84
DP-100LN1	0.025	0.62	1.17	0.022	0.007	23.38	7.45	2.24	0.015	0.023	100
DP-100LN2	0.021	0.65	1.18	0.021	0.007	23.87	3.52	2.42	0.017	0.017	100

Thickness : 12mm
* : After GTA welding (Point count method : ASTM E562)

2.2 Hot cracking test

The values of BTR were measured by the Trans-Varestraint test except for SUS304L. The procedure of the Trans-Varestraint test is shown elsewhere[8]. The value of BTR of SUS304L was measured by MISO technique[9,10].

3. Modelling Used

The modeling used was completely the same as in the previous paper[1], including assumptions, growth conditions of the solid-liquid interface and physical constants*.

The value of BTR was determined as follows: In the modelling, the solid-liquid interface advances so that the liquidus temperature of the liquid may agree with the actual temperature. Impurities are enriched into residual liquid with the advance, and the temperature where the last mesh enriched with impurities solidifies gives the solidus temperature. On the other hand, as mentioned in the introduction, the fractograph of solidification crack by the Trans-Varestraint test implied[4,5] that the lower temperature limit of BTR corresponded to the temperature where small amount of residual liquid enriched with impurities solidified completely. Namely, it is guessed that the lower temperature limit of BTR has the same meaning as the temperature where the last mesh solidifies. Therefore, BTR was calculated as the difference between the initial liquidus temperature which was measured experimentally and the temperature where the last mesh solidifies.

Concerning SUS316L and SUS304L where peritectic/eutectic reaction occurs, BTR was not calculated. Only the incipient temperature of peritectic/eutectic reaction was calculated as follows: N. Suutala classified the solidification mode into four types[12], namely A, AF, FA and F modes, where A and F mean austenite and ferrite phase respectively. The mode AF means that austenite is primary phase and ferrite solidifies as subsequent phase by peritectic/eutectic reaction. The mode FA has a reverse meaning of the AF mode. The demarcation between AF and FA solidification modes is expressed as $Cr_{eq}/Ni_{eq} = 1.52$[12], where Cr_{eq} and Ni_{eq} are those proposed by Ö. Hammar *et al.*[13]. Therefore, when the Cr_{eq}/Ni_{eq} ratio calculated crossed the demarcation, it was judged

*: According to the results in the previous paper[1], 0.92 rather than 0.88 was suitable for the partition coefficient of Cr in austenite solidification. However, 0.88 which is quoted from T. Okamoto *et al.*[11] was used in this paper, because the effect of partition coefficient of Cr on BTR was very small.

that peritectic/eutectic reaction occurred, and its temperature was printed out.

4. Results and Discussion

4.1 Effect of total number of division on BTR calculated

For the purpose of this paper, the optimum mesh size should be established, because the accuracy largely depends on the size. In the modelling used, one volume element is divided by n_x in x direction and n_y in y direction (see Fig. 1 (c) in the previous paper[1]). Namely, one mesh size is in inverse proportion to $n_x \times n_y$ ($n_x = n_y$ at the present). In this paper, $n_x \times n_y$ is named the total number of division N_T.

Figure 1 shows the effect of N_T on BTR calculated for SUS430 and SUS310S. Their experimental BTR are also given. The BTR calculated for SUS430 saturates easily, and the saturated value well agrees with the experimental value. The reason of easy saturation is because of relatively higher partition coefficient and relatively faster diffusivity of solute elements for primary ferrite phase. To get the saturated value, N_T should be 200 at least. On the other hand, the BTR calculated for SUS310S saturates very slowly, and the nearly saturated value at N_T of 600 is too large compared with the experimental value. This disagreement can be explained as follows: A typical microstructure near the lower temperature limit of BTR in SUS310S is shown in **Fig. 2**. It is noticed that solidification was finished by the formation of inclusion at the intersectional site of the primary and the secondary dendrite arm boundaries, which was enriched with P, S etc. according to EDX results. This implies that the residual liquid having nearly the same size as the inclusion was the smallest unit which solidified at a time finally because of e.g. eutectic reaction to form inclusion. This

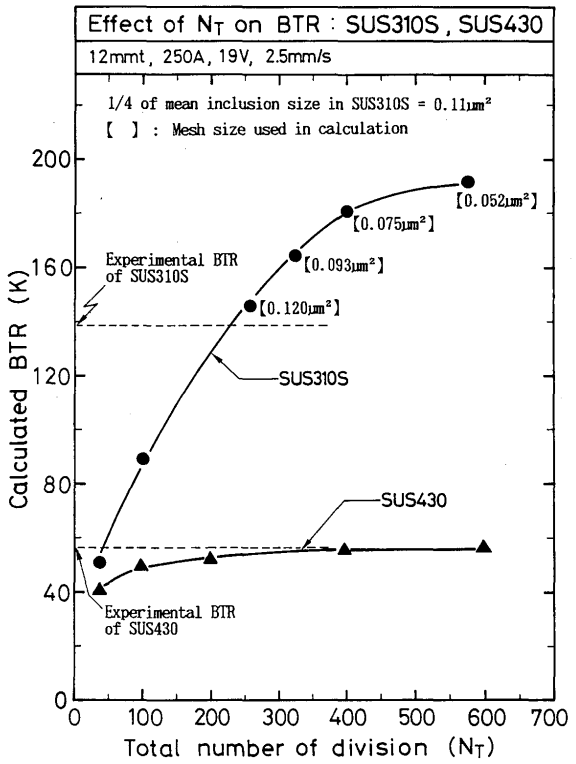

Fig. 1 Effects of total number of division on calculated BTR of SUS310S and SUS430.

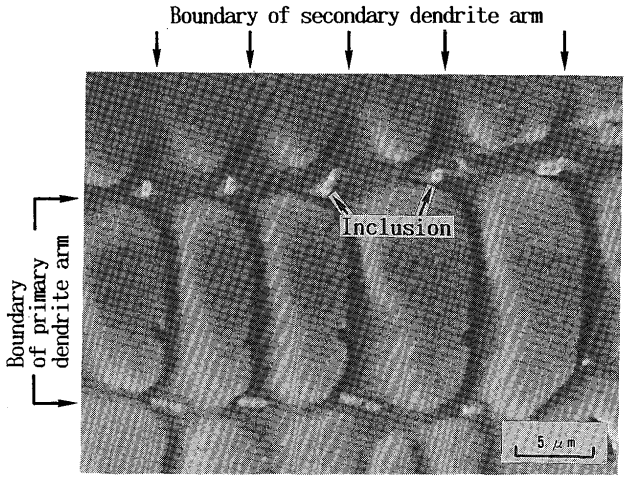

Fig. 2 Typical microstructure near the lower temperature limit of BTR in SUS310S.

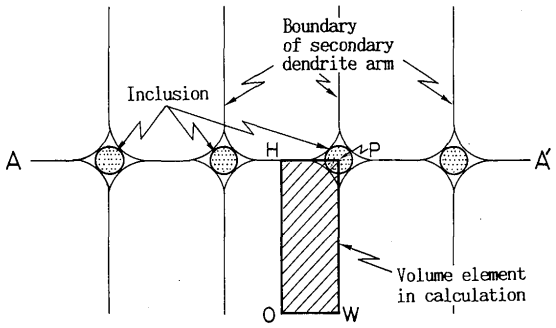

AA' : Boundary of primary dendrite arm

(a) Location of inclusion and volume element

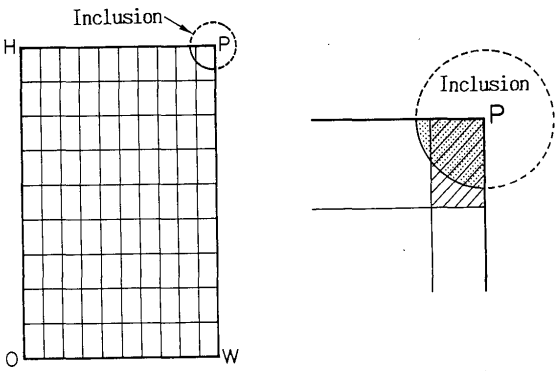

(b) Comparison between a mesh and inclusion size

(c) Details near P in (b)

Fig. 3 Schematic illustration of relationship between mean inclusion and a mesh size for determination of total number of division in calculation of BTR in SUS310S

further suggests that the calculation in the modelling should be stopped when the size of residual liquid get nearly the same size as the inclusions. In the model, as shown in **Fig. 3 (a)**, it is noticed that one volume element occupies 1/4 of each inclusion. Therefore, the easiest way to deal with this problem is to make one mesh size correspond to 1/4 of mean inclusion size as shown in Fig. 3 **(b)** and **(c)**, where the dotted zone means 1/4 of mean inclusion size and the dashed zone means one mesh. On the other hand, quantitative measurement gave about $0.11\mu m^2$ as 1/4 of mean inclusion size. Noticing Fig. 1 again, the numeral in parentheses means one mesh size, and it is seen that the mesh size in the case of N_T larger than about 320 is too small compared with the 1/4 value of inclusion size. Interestingly, N_T of about 260 (exactly 256) gives the mesh size of $0.12\mu m^2$ which is nearly the same as the 1/4 value of inclusion size, and the BTR calculated well agrees with the experimental value.

Therefore, it is understood that for materials where inclusions are definitely formed in final stage of solidification the selection of optimum mesh size or total number of division is important. For example, although N_T of 256 was optimum for commercial SUS310S used in Fig. 1, N_T of 400 was optimum for experimental SUS310S where S and P content is much lower (P < 0.007%, S < 0.009%).

4.2 Further confirmation and ranking of harmful elements

4.2.1 Further confirmation of applicability to BTR estimation

About 10 years ago, some of the authors[14–16] already studied BTR of many kinds of SUS310S by changing P and S content widely. These data and one datum of SUS430[16,17] were numerically analyzed in this paper by the modelling in order to get further confirmation of the applicability of the modelling to BTR estimation. The calculated and the experimental BTR are plotted in **Fig. 4**, where only two data denoted by asterisk are the data quoted from the previous paper[8]. The correspondence between the calculated and the experimental BTR is good inspite of widely changed P, S and Si contents and irrespective of primary solidification phase.

Then, the applicability to SUS304L and SUS316L was studied, which are well known to have peritectic/eutectic reaction during solidification[17,18]. According to the previous paper[6,7], SUS304L in Table 1 solidifies with primary ferrite and subsequent austenite by peritectic/eutectic reaction, and SUS316L in Table 1 solidifies with primary austenite and subsequent ferrite by peritectic/eutectic reaction. As mentioned already, the calculation in the modelling was stopped when peritectic/eutectic reaction started. The calculated temperatures and the experimental ones[6,7] are compared in **Fig. 5**, where ΔP/E means the temperature difference from liquidus to the incipient temperature of peritectic/eutectic reaction. It is noticed that the correspondence in the incipient temper-

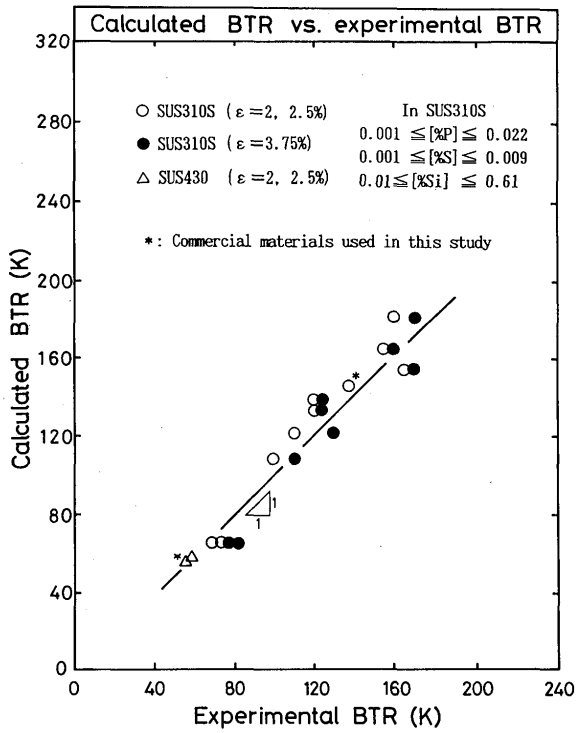

Fig. 4 Comparison between calculated and experimental BTR of SUS310S and SUS430. The data with asterisk were obtained in the previous paper[8]. The others were quoted from ref.[14–16].

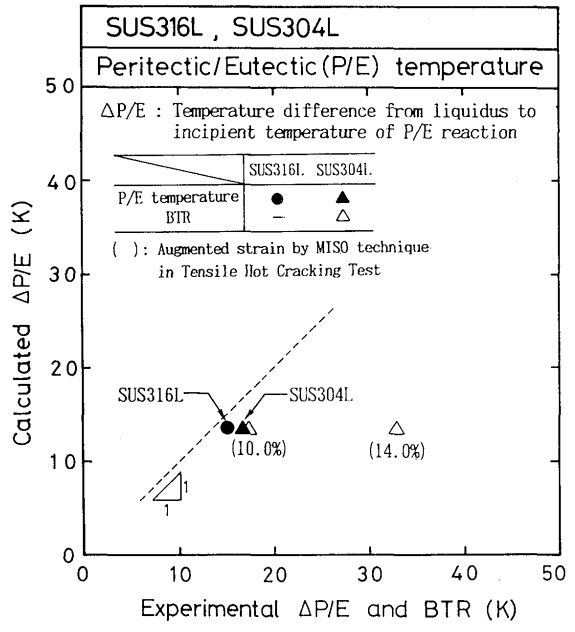

Fig. 5 Comparison between calculated and experimental temperature difference from liquidus to incipient temperature of paritectic/eutectic reaction, and BTR.

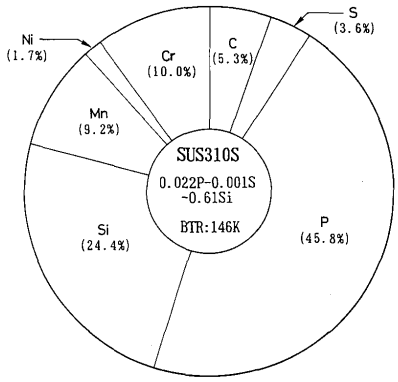

(a) High P – Low S

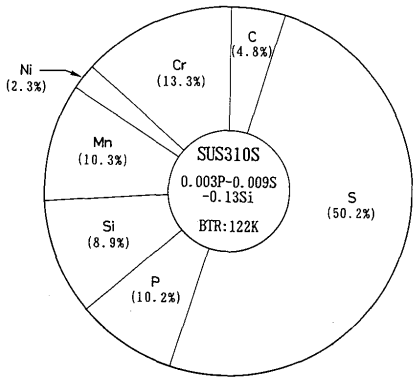

(b) Low P – High S

Fig. 6 Contribution of elements to calculated BTR in SUS310S

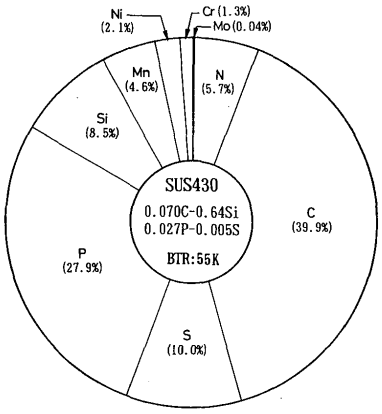

Fig. 7 Contribution of elements to calculated BTR in SUS430

ature of peritectic/eutectic reaction between the calculation and the experiment is very good. The open triangles in Fig. 5 mean the BTR of SUS304L[10], and the numerals in the parenthesis mean augmented strain measured by MISO technique in Tensile Hot Cracking test. It is shown[9] that the strain measured by MISO technique gives much bigger value than that evaluated by t/2R in the Trans-Varestraint test (t: specimen thickness, R: radius of curvature of the bending block). If the augmented strain is 10%, BTR almost agree with the incipient temperature of peritectic/eutectic reaction. This is because residual liquid is confined inside of austenite phase, and thus crack propagation is stopped at this temperature[17,19]. If the augmented strain is 14%, however, BTR is much larger. This is because crack propagates along austenite-ferrite boundary[17,19].

Therefore, for the material such as SUS304L and SUS316L, the modelling is useful for only the estimation of the incipient temperature of peritectic/eutectic reaction, and is not necessarily useful for the estimation of BTR. Improving of the modelling or advanced modelling should be required for these materials.

4.2.2 Ranking of harmful elements

In the modelling, BTR has the same meaning as total melting point depression from the initial liquidus temperature, and the total depression is expressed as the sum of the partial depression by each element. This means that the ranking of harmful elements is easily possible by comparing the partial depression to total depression (BTR) ratio, namely the contribution of each element.

One example of the contributions of elements in SUS310S shown in Fig. 1 is given in **Fig. 6 (a)**. Another example is shown in **(b)**, where the P content is much lower, the S content is higher and Si content is lower than (a). From these two figures, it is seen that S and P and then Si are strongly contributory elements. This tendency has been well known through many experimental results[14,20,21].

Figure 7 shows the contributions of elements in SUS430 shown in Fig. 1. In this result, the contribution of nitrogen was calculated on the same basis which will be shown in 4.3. In this composition, C is the most contributory, secondary P and then S. By the way, D.H. Kah *et al.*[22] reported that S, C, N and P are the primary contributors to hot cracking in SUS430 by the Trans-Varestraint test. Although they derived this result from the measurement of total crack length, both of the calculated and their experimental results have a good agreement.

4.3 Applicability to duplex stainless steel and contribution of nitrogen

4.3.1 Prediction of harmful effect of nitrogen

The BTR of base metal and deposited metals of duplex stainless steel was calculated by the same manner as used for SUS310S and SUS430, and the results are listed in **Table 3**. It is seen that the calculated BTR is too small compared with the experimental BTR.

The authors considered that this discrepancy is due to the neglect of the harmful effect of nitrogen by the next two reasons: (1) According to Fig. 7 for SUS430 whose

Table 3 Comparison between experimental and calculated BTR without taking account of nitrogen in SUS329J2L and its deposited metals

Material	Experimental BTR (K)	Calculated BTR (K)
Base metal	98	61
DP-70HN	95	63
DP-80HN	95	70
DP-100HN	120	61

DP : Deposited metal

solidification mode is the same as duplex stainless steel[6,23], carbon has the biggest contribution to BTR. Such harmful effect of carbon is reported by D.H.Kah *et al.*[22], too. Considering that nitrogen is an austenite stabilizer as well as carbon concerning solidification mode, it can be estimated that nitrogen should be harmful, too. (2) Nitrogen content in duplex stainless steel is very high compared with general austenitic and ferritic stainless steel.

Therefore, the authors tried to take account of nitrogen in BTR calculation. However, it is difficult to get the values of partition coefficient and liquidus gradient*, because even new Fe-N phase diagram[24] does not give any information around Fe corner.

With the above reason, the authors decided to deal with this problem approximately. The authors noticed that nitrogen is ressemble to carbon not only in austenite stabilization but also in interstitial element. This implies that the effect of nitrogen may be dealed as one kind of carbon equivalent. Namely, the carbon content used in the calculation of BTR might be substituted by C_{eq} which is difined by the next equation.

$$C_{eq} = [\%C] + a_N [\%N] \quad \cdots\cdots (1)$$

where a_N is the coefficient to get effectiveness of nitrogen.

Therefore, the problem is how to determine the value of a_N. Referring to the equations of C_{eq} which have been proposed until now to estimate the microstructure at room temperature. W.T. DeLong *et al.*[26] gave a_N of 1.0 and Ö. Hammar *et al.*[13] gave a_N of 0.65. N. Suutala[12] showed that Hammar's C_{eq} fits well with the solidification mode of stainless steel containing relatively high amount of nitrogen. However, exact evaluation of the a_N value is not clear, and thus a_N = 0, 0.65 and 1 were tried in this study. **Figure 8** campares the calculated and the experimental results. It is seen that taking account of the effect of nitrigen improves the correlation between the calculated and the experimental BTR, and that the a_N value of 1.0 was the best, although the scattering is not very small.

Therefore, in this study the effect of nitrogen was taken account of by the carbon equivalent with a_N = 1, which is expressed by the simple sum of [%C] and [%N]. According to this treatment, the contribution of nitrogen to BTR is very big as seen in **Fig. 9**.

4.3.2 Experimental confirmation of harmful effect of nitrogen

*: Basic Open Hearth Steelmaking[25] gives the partition coefficient of 0.25 in δ-Fe, but its authority is not given.

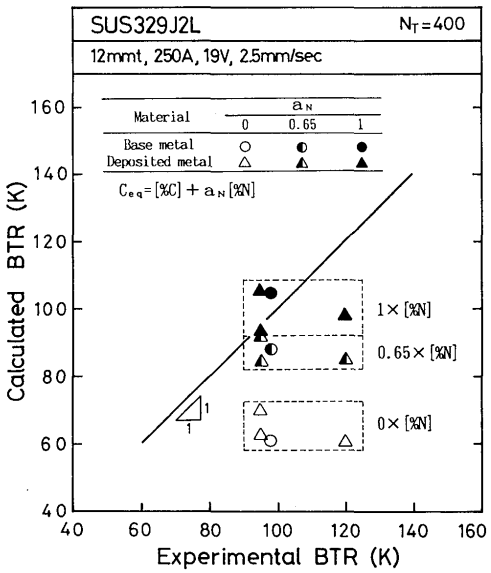

Fig. 8 Comparison between experimental and calculated BTR with taking account of nitrogen content in calculation

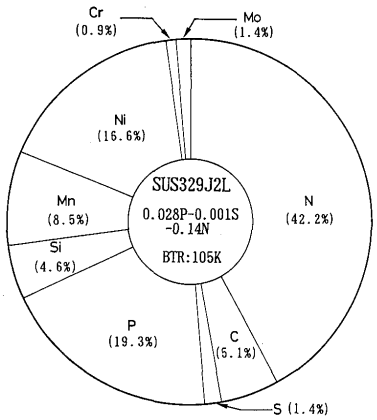

Fig. 9 Contribution of elements to calculated BTR in SUS329J2L

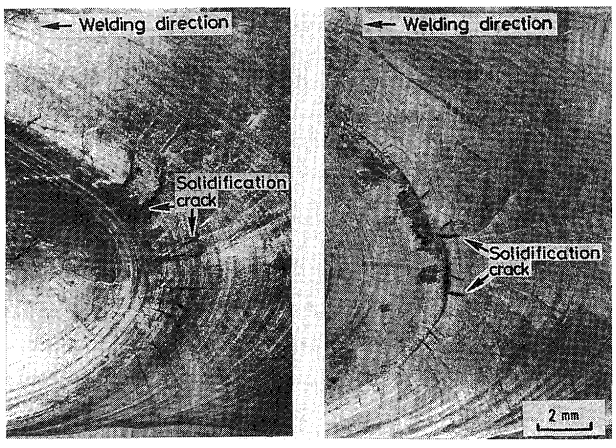

Fig. 10 Typical macrostructures in weld surface after the Trans-Varestraint test
(a) DP-70HN (0.11%N, δ: 77%)
(b) DP-100LN1 (0.02%N, δ: 100%)

Tentative deposited metal whose nitrogen content was 0.02 to 0.04% and ferrite content was varied from about 0 to 100% was tested by the Trans-Varestraint test. Typical macrostructures after the test are shown in **Fig. 10**, and it is seen that the maximum crack length is shortened by lowering nitrogen content. Moreover, it is seen that the degree of crack opening is decreased by lowering nitrogen content, and this implies that lowering nitrogen content increases the minimum ductility required for crack formation.

Figure 11 summarizes the maximum and the total crack lengths vs. ferrite content together with the data shown in the previous paper[8] which contain 0.10 to 0.14% nitrogen. In the range of ferrite content less than about a few percentage, namely in the range of primary austenite solidification (A mode[12]), the effect of nitrogen is not seen. This should be reasonable because nitrogen is austenite stabilizer. In the range of ferrite content higher than about 80%, a beneficial effect of reducing nitrogen content is clearly seen. It should be noticed that both the maximum and the total crack lengths of these low nitrogen deposited metal are almost the same as those of SUS430 base metal. Therefore, a harmful effect of nitrogen in the solidification mode in which ferrite is the primary phase was confirmed experimentally.

Figure 12 shows the calculated BTR for the representative materials shown in Fig. 11. The data with parentheses mean that calculation of BTR was stopped when the temperature reached the incipient temperature of peritectic/eutectic reaction as mentioned in Fig. 5. As a whole, the tendency obtained by calculation agree well with the experimental tendency.

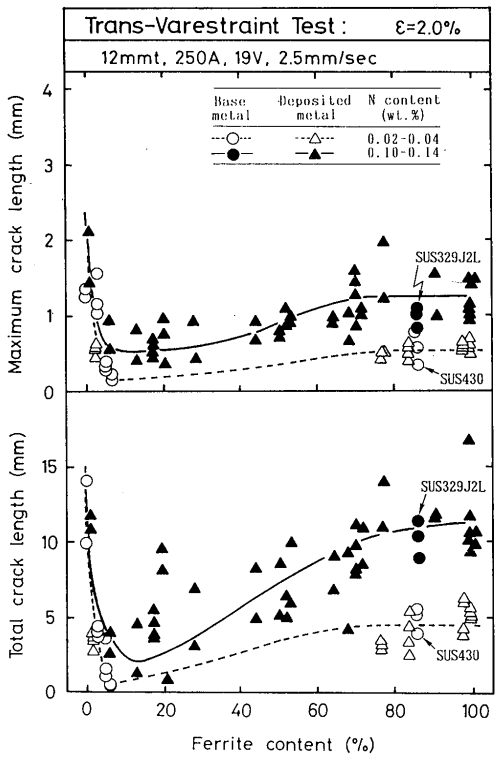

Fig. 11 Maximum and total crack lengths vs. ferrite content under two levels of nitrogen content.

5. Conclusion

Two dimensional modelling of the cellular dendrite growth during weld solidification was applied to predict Solidification Brittleness Temperature Range (BTR) of several kinds of stainless steels. Moreover, the modelling was utilized to predict the reason why duplex stainless steel has a relatively large BTR, and the prediction was confirmed experimentally.

Main conclusions obtained are as follows:

(1) The calculated BTR for ferritic stainless steel agreed well with the experimental BTR unconditionally.

(2) The calculated BTR for fully austenitic stainless steel agreed well with the experimental BTR by making mesh size for numerical analysis nearly equal to the size of inclusions, because interdendritic inclusions are easily formed in this type of material because of small partition coefficient and slow diffusivity in solid for impurities.

(3) It is easy to rank harmful elements by the modelling. According to the calculated results, the primary contributor to BTR is P, S and then Si in fully austenitic stainless steel, and is C, S and P in ferritic stainless steel.

(4) For austenitic stainless steels where peritectic/eutectic reaction occurs, the incipient temperature of the reaction can be well predicted by the modelling.

(5) Application of the modelling to duplex stainless steel showed that the calculated BTR was too small compared with the experimental BTR if calculation is done without taking account of nitrogen. Moreover, it was

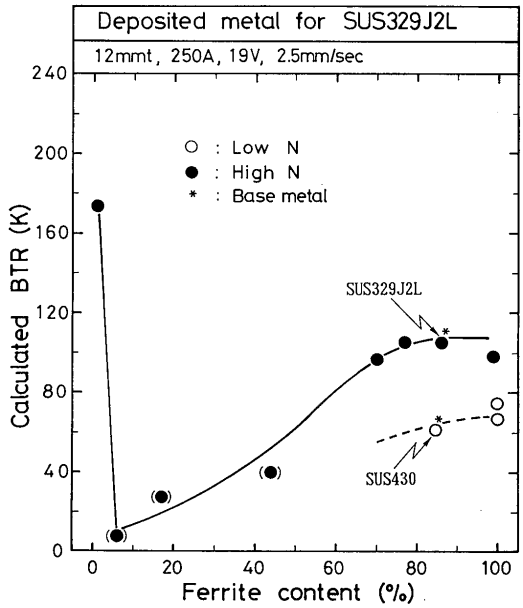

Fig. 12 Calculated BTR vs. ferrite content under two levels of nitrogen content.

shown that the prediction of BTR is roughly possible by substituting the sum of [%C] and [%N] to [%C] in the modelling.

(6) The harmful effect of nitrogen was confirmed experimentally by making tentative deposited metals containing low nitrogen. According to these calculated and experimental results, the contribution of nitrogen to BTR in duplex stainless steel is crucial.

(7) Additional calculation including the results from (1) to (6) could explain well the tendency of crack susceptibility of stainless steels where ferrite content was widely changed as well as nitrogen content.

Acknowledgement

The authors would like to thank Mr. T. Hirose, and M. Yamamoto, formerly students of Kinki Univ., for their cooperation in the experiment, and Sumikin Welding Industries, Ltd., for its supply of materials used.

Reference

1) F. Matsuda, H. Nakagawa and J.B. LEE: Trans. of JWRI, **18**-1 (1989), 107–117.
2) W.F. Savage and C.D. Lundin: Welding J., **44**-10 (1965), 433s–442s.
3) T. Senda, F. Matsuda, G. Takano, K. Watanabe, T. Kobayashi and T. Matsuzaka: Trans. of JWS, **2**-2 (1971), 1–22.
4) F. Matsuda, H. Nakagawa, S. Ogata and S. Katayama: Trans. of JWRI, 7-1 (1978), 59–70.
5) F. Matsuda and H. Nakagawa: Trans. of JWRI, 8-1 (1979), 155–157.
6) F. Matsuda, H.Nakagawa and J.B. LEE: Trans. of JWRI, **16**-2 (1987), 115–121.
7) F. Matsuda, H. Nakagawa and J.B. LEE: Quarterly J. of JWS, 7-2 (1989), 229–234 (in Japanese).
8) F. Matsuda, H. Nakagawa, I. Kato and Y. Murata: Trans. of JWRI, **15**-1 (1986), 99–112.
9) F. Matsuda, H. Nakagawa, K. Nakata, H. Kohmoto and Y. Honda: Trans. of JWRI, **12**-1 (1983), 65–72.
10) F. Matsuda, H. Nakagawa, H. Kohmoto, Y. Hondo and Y. Matsubara: Trans. of JWRI, **12**-1 (1983), 73–80.
11) T. Okamoto, K. Kishitake and K. Murakami: Trans. ISIJ, **21** (1981), 641–648.
12) N. Suutala: Metal. Trans., **13A**-12 (1982), 2121–2130.
13) Ö. Hammar and U. Svensson: "Solidification and Casting of Metals", The Metals Society, London, (1979), 401–410.
14) F. Matsuda, S. Katayama and Y. Arata: Trans. of JWRI, **6**-1 (1977), 105–116.
15) Y. Arata, F. Matsuda, H. Nakagawa and S. Katayama: Trans. of JWRI, 7-2 (1978), 21–24.
16) S. Katayama: Ph. D. Thesis, Osaka University, Japan (1981) (in Japanese).
17) F. Matsuda, H. Nakagawa, T. Uehara, S. Katayama and Y. Arata: Trans. of JWRI, 8-1 (1979), 105–112.
18) N. Suutala, T. Takalo and T. Moisio: Metal. Trans., **11A**-5 (1980), 717–725.
19) F. Matsuda, H. Nakagawa, S. Katayama and Y. Arata: Trans. of JWRI, **13**-2 (1982), 41–58.
20) R.S. Brown and J.B. Koch: Welding J., **57**-2 (1978), 38s–42s.
21) J.C. Lippold and W.F. Savage: Welding J., **61**-2 (1982), 388s–396s.
22) D.H. Kah and D.W. Dickinson: Welding J., **60**-8 (1981), 135s–142s.
23) F. Matsuda, H. Nakagawa and J.B. LEE: Quarterly J. of JWS, 7-2 (1989), 235–239 (in Japanese)
24) T.B. Masaalski: "Binary Alloy Phase Diagrams" ASM (1986)
25) AIME, "Basic Open Hearth Steelmaking", (1964).
26) W.T. DeLong, G.A. Ostrom and E.R. Szumachowski: Welding J., **35** (1956), 526s–532s.